GEOLOGY | THE GEOLOGICAL SOCIETY OF AMERICA®

https://doi.org/10.1130/G47022.1

Manuscript received 18 September 2019
Revised manuscript received 9 December 2019
Manuscript accepted 18 December 2019

Published online 31 January 2020

Distributed ductile thinning during thrust emplacement: A commonly overlooked exhumation mechanism

Sean P. Long[1]* and Matthew J. Kohn[2]
[1]School of the Environment, Washington State University, Pullman, Washington 99164, USA
[2]Department of Geosciences, Boise State University, Boise, Idaho 83725, USA

ABSTRACT

Quantifying the processes that control exhumation is essential for understanding the evolution of mountain belts. In the Cordilleran orogen in Nevada (western United States), rocks exhumed in the Ruby–East Humboldt metamorphic core complex underwent 4 ± 2 kbar of decompression between 85 and 60 Ma, which has been interpreted as a consequence of synorogenic extension. However, evidence for significant normal faulting in this region prior to 45 Ma is lacking. Here, we present an alternative interpretation: that this decompression can be attributed to distributed ductile thinning (DDT) of mid-crustal metamorphic rocks above the basal Cordilleran décollement during eastward translation. Such a process has been documented within the Himalayan Main Central thrust sheet, which locally accommodated up to 15 km of DDT during Miocene translation. Other examples of DDT have been documented in the Alpine and Caledonian orogens (Europe), and the Sanbagawa belt (Japan). DDT may represent a widespread exhumation process that can account for a significant portion of the decompression path of deeply exhumed rocks. As a condition of strain compatibility, thrust-parallel stretching accompanying DDT is expected to enhance displacement magnitude in the transport direction, and is therefore an important component of the deformation field that must be considered for accurate assessment of mass balance in thrust systems.

INTRODUCTION

Understanding the relative contributions of processes that exhume rocks during and after orogenesis is critical for elucidating the complete cycle from construction to dismemberment of an orogen (e.g., England and Molnar, 1990; Ring et al., 1999). Exhumation in mountain belts is generally attributed to two primary processes (Fig. 1A): stream erosion that becomes enhanced as elevations increase during crustal thickening, and tectonic denudation of the footwalls of normal faults and detachment systems (e.g., Wernicke and Burchfiel, 1982; Platt, 1993; Willett and Brandon, 2002). However, a third potential exhumation process, distributed ductile thinning (DDT) during contractional deformation, has received considerably less attention (e.g., Feehan and Brandon, 1999; Ring et al., 1999; Ring and Kassem, 2007). Here, we argue for the importance of this exhumation mechanism by highlighting case studies of DDT within thick, hot orogens including the North American Cordillera and the Himalaya. The occurrence of DDT has global implications for the relative importance of synorogenic exhumation processes, and for accurate quantification of orogenic mass balance.

DISTRIBUTED THINNING IN THE NORTH AMERICAN CORDILLERA IN NEVADA, USA

The Conundrum of Late Cretaceous Decompression

The North American Cordillera was constructed between the Jurassic and Paleogene in response to interplate coupling induced by Andean-style subduction (e.g., DeCelles, 2004). At the latitude of Nevada and Utah (western United States), the majority of Cordilleran upper-crustal shortening (150–220 km) was accommodated in the frontal Sevier fold-thrust belt between ca. 150 and ca. 50 Ma (e.g., DeCelles, 2004; Yonkee and Weil, 2015) (Fig. 1B). This fold-thrust belt projects westward under Nevada and is interpreted to have rooted into a master shear zone located at or beneath the contact between Neoproterozoic sedimentary rocks and Archean–Proterozoic crystalline basement (e.g., Miller and Gans, 1989).

By the Late Cretaceous, eastern Nevada was likely a high-elevation plateau with 50–60-km-thick crust (e.g., Coney and Harms, 1984). Between 70 and 90 Ma, this hinterland plateau experienced widespread granitic magmatism (e.g., Miller and Gans, 1989; Long and Soignard, 2016), which has been attributed to lower-crustal anatexis triggered by lithospheric delamination (Wells and Hoisch, 2008). Magmatism was contemporary with peak metamorphism recorded in mid-crustal rocks that are now exhumed within several core complexes, including in the Ruby–East Humboldt core complex (REH) between ca. 89 and ca. 77 Ma (McGrew et al., 2000; Hallett and Spear, 2014, 2015). Pressure-temperature-time (*P-T-t*) paths from REH rocks define cooling and decompression from ~800 °C and ~8–11 kbar to ~650 °C and ~5–6 kbar between ca. 85 and ca. 60 Ma, and to ~500–550 °C and ~3–4 kbar between ca. 50 and ca. 28 Ma (McGrew et al., 2000; Henry et al., 2011; Hallett and Spear, 2014, 2015).

The early (ca. 85–60 Ma) decompression recorded in the REH has been interpreted as the consequence of extension of the middle and upper crust, which was coeval with shortening in the Sevier fold-thrust belt (Hodges et al., 1992; McGrew et al., 2000; Wells and Hoisch, 2008). However, field relationships in the region surrounding the REH (summarized by Henry et al. [2011]) indicate minimal (if any) normal faulting before ca. 45 Ma, which has generated a long-standing debate over the processes responsible for Late Cretaceous decompression. Only a single pre-Eocene normal fault has been reported from this region, 45 km to the east of the REH (Camilleri and Chamberlain, 1997). Low-temperature thermochronometry and a lack of differential tilting between Eocene volcanic rocks and Miocene sedimentary rocks indicate that the inception of widespread normal faulting in this

*E-mail: sean.p.long@wsu.edu

CITATION: Long, S.P., and Kohn, M.J., 2020, Distributed ductile thinning during thrust emplacement: A commonly overlooked exhumation mechanism: Geology, v. 48, p. 368–373, https://doi.org/10.1130/G47022.1

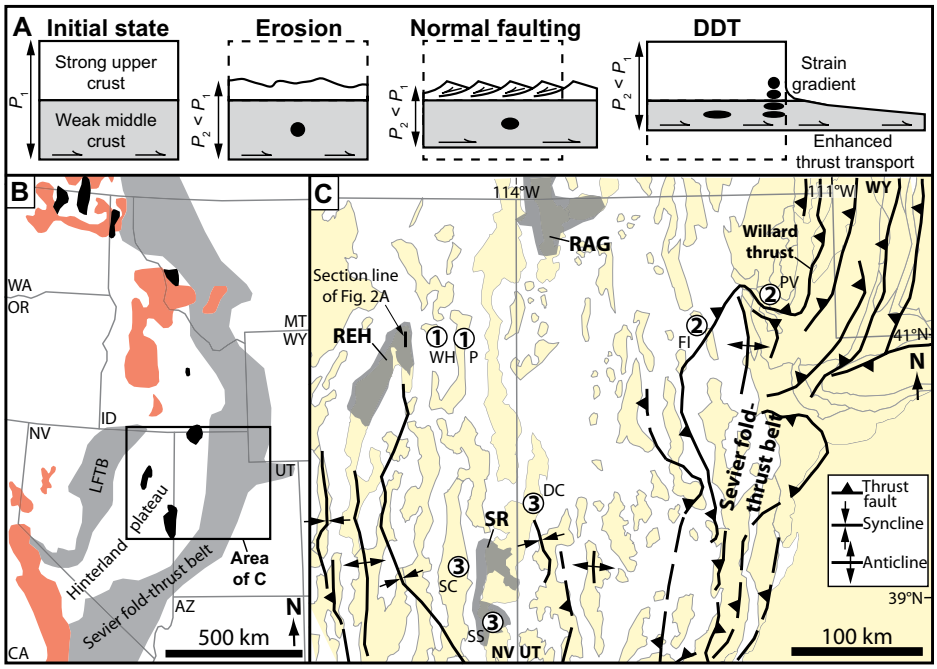

Figure 1. (A) Schematic diagrams illustrating three different exhumation processes that can operate during orogenesis (P_1 = initial pressure, P_2 = pressure after exhumation), including erosion, tectonic denudation accompanying normal faulting, and distributed ductile thinning (DDT). Schematic strain ellipses are shown for each process. (B) Map of major components of western United States portion of Cordilleran orogen (modified from DeCelles, 2004). Red polygons are Cordilleran magmatic arc rocks, black polygons are metamorphic core complexes, and "LFTB" is Luning-Fencemaker thrust belt. (C) Map of northeastern Nevada and northern Utah showing ranges in yellow (polygons from McQuarrie and Wernicke, 2005), metamorphic core complexes in dark gray (REH—Ruby–East Humboldt; RAG—Raft River–Albion–Grouse Creek; SR—Snake Range), and Cordilleran contractional structures. Numbered localities correspond to documented sites of distributed subhorizontal stretching and subvertical thinning during Cordilleran contractional deformation, including: 1—Wood Hills (WH) and Pequop Mountains (P) (Camilleri, 1998); 2—basal portion of Willard thrust sheet at Fremont Island (FI) and Pineview area (PV) (Yonkee, 2005); 3—Deep Creek (DC), Schell Creek (SC), and Southern Snake (SS) ranges (Miller and Gans, 1989). WA—Washington; OR—Oregon; NV—Nevada; CA—California; ID—Idaho; MT—Montana; WY—Wyoming; UA—Utah; AZ—Arizona.

region was no earlier than the middle Miocene (Colgan et al., 2010; Henry et al., 2011).

Evidence in Support of Distributed Ductile Thinning

In the northeastern part of the REH, *P-T-t* paths determined from samples collected from two structural domains—the Lizzies Basin block in the south, and the Winchell Lake nappe in the north (Fig. 2)—demonstrate similar exhumation histories (McGrew et al., 2000; Hallett and Spear, 2014). These samples were collected from a 1.5 km total structural thickness (Fig. 2A), and they lie below the interval of deformation associated with the overlying, top-down-to-west, extensional mylonitic shear zone that exhumed the REH between the Eocene and Miocene (Henry et al., 2011). *P-T-t* paths from these rocks (Fig. 2B) (Hallett and Spear, 2015) define significant condensing of structural levels between the Late Cretaceous and Paleocene (Fig. 2C). During attainment of peak pressures, which occurred between ca. 89 and 78 Ma in the Lizzies Basin block and ca. 83 and 77 Ma in the Winchell Lake nappe, rocks that now compose this 1.5-km-thick interval spanned between ~8 and ~11.5 kbar, corresponding to an original thickness range of 7–13 km. By ca. 59–61 Ma, rocks in both the Lizzies Basin block and Winchell Lake nappe had been exhumed to a relatively narrow pressure range of ~5–6.5 kbar, indicating a general condensing of these rocks into a narrower (4–6 km) structural thickness range.

Migmatitic rocks are abundant in the Lizzies Basin block and Winchell Lake nappe, and both of these structural domains underwent deformation and initial exhumation in the presence of melt (McGrew et al., 2000; Hallett and Spear, 2014). Following widespread leucogranite generation at ca. 85 Ma (Henry et al., 2011), melt crystallization in the Lizzies Basin block initiated by 80 Ma, and melt was present for at least the earliest period of decompression (Hallett and Spear, 2015). Melt crystallization in the Winchell Lake nappe spanned from 77 to 59 Ma, with melt likely present for a significant fraction of the decompression path (Hallett and Spear, 2015). Partial melting greatly enhanced the potential for ductile flow, promoting high-strain penetrative stretching and thinning (e.g., Rosenberg and Handy, 2005). In the Winchell Lake nappe, Neoproterozoic to Mississippian sedimentary units of the Cordilleran passive margin basin were ductilely thinned from an original stratigraphic thickness of ~8 km (Colgan et al., 2010) to only a few hundred meters (McGrew et al., 2000; Henry et al., 2011) (Fig. 2A), and in the Lizzies Basin block, ductile thinning of Neoproterozoic–Cambrian rocks reduced their structural thickness to ~1.5 km (McGrew et al., 2000). This corresponds to ~80%–95% vertical thinning.

Based on the evidence for condensing of structural levels, melt-present deformation during exhumation, and extreme attenuation of stratigraphic units, we propose that distributed subhorizontal stretching and subvertical thinning of mid-crustal rocks above the basal Sevier décollement best explains the 4 ± 2 kbar of decompression documented in the REH between ca. 85 and ca. 60 Ma (Fig. 3). We propose that this mid-crustal strain was kinematically linked to shortening in the Sevier fold-thrust belt (discussed below), which may solve the conundrum of missing pre-Eocene normal faulting in northeastern Nevada.

Observations from deeply exhumed rocks in the surrounding region of Nevada and Utah highlight additional evidence for distributed subvertical thinning during Cretaceous east-vergent translation above the basal Sevier décollement (Fig. 1C). In the Wood Hills and Pequop Mountains, 20–45 km to the east of the REH, greenschist- and amphibolite-facies metasedimentary rocks accommodated as much as 30%–50% bedding-subparallel, pure shear–dominated flattening (estimated by comparison to stratigraphic thicknesses in surrounding ranges) during Cordilleran prograde metamorphism at paleodepths of 15–25 km (Camilleri, 1998). To the east in the Sevier thrust belt, the basal 5 km of the Willard thrust sheet experienced thrust-subparallel stretching and as much as 50% thrust-normal thinning at paleodepths of 10–15 km and deformation temperatures of 300–400 °C (Yonkee, 2005). In the Deep Creek, Schell Creek, and Snake Ranges, 150–200 km to the southeast of the REH, Miller and Gans (1989) documented east-vergent shear fabrics that illustrate a downward-increasing component of pure shear–dominated, subvertical thinning. They interpreted these fabrics to represent distributed shear above the basal Sevier décollement at paleodepths of 8–12 km.

These studies provide evidence that much of the Cordilleran middle crust was undergoing DDT (Fig. 3B), which contributed to decompression of the REH rocks to ~5–6.5 kbar (~19–25 km depths) by ca. 60 Ma. Therefore, in addition to experiencing significant internal thinning, the REH rocks were also exhumed by DDT of overlying mid-crustal rocks. The ~80%–95%

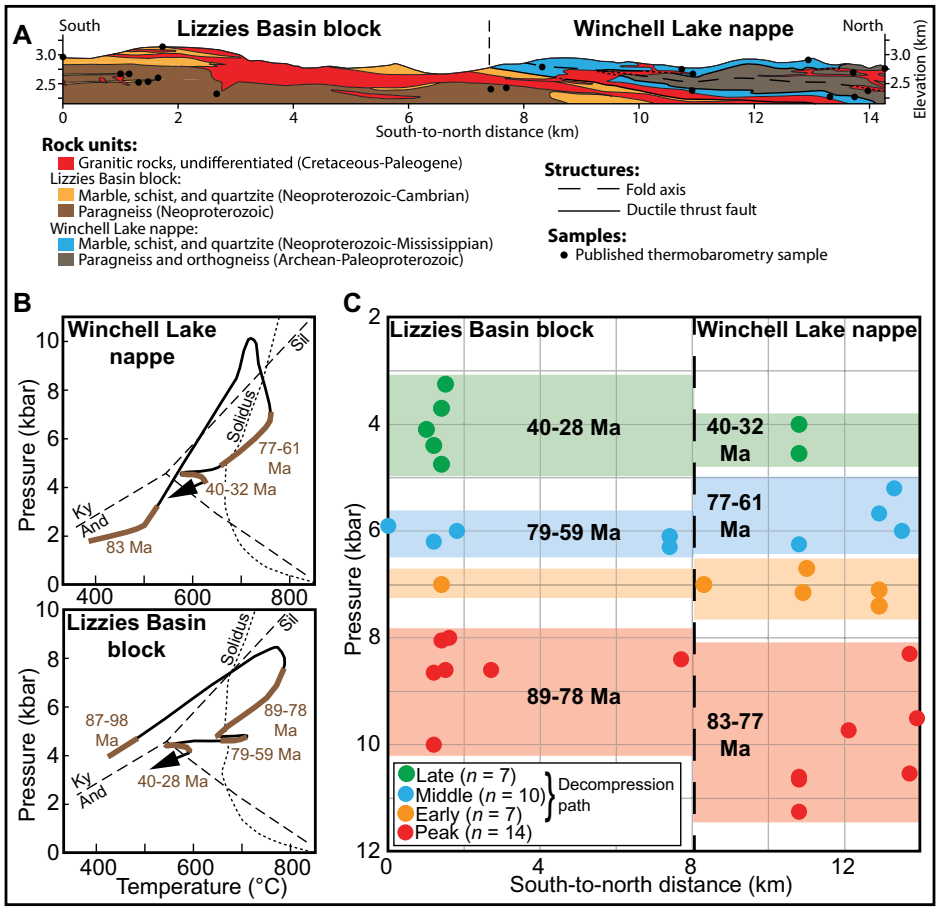

Figure 2. (A) Cross section of northern East Humboldt Range, Nevada, United States (no vertical exaggeration; modified from Hallett and Spear [2014]; see the GSA Data Repository[1] for a more detailed version), illustrating the deformation geometry of the Lizzies Basin block and Winchell Lake nappe, and extreme ductile thinning of Neoproterozoic–Mississippian rocks in the Winchell Lake nappe. Locations of published thermobarometry samples from Hodges et al. (1992), Peters and Wickham (1994), McGrew et al. (2000), and Hallett and Spear (2014) are projected onto the cross section. (B) Pressure-temperature-time paths for the Winchell Lake nappe and Lizzies Basin block showing timing constraints from monazite and zircon geochronology (simplified from Hallett and Spear, 2015). Ky—kyanite; Sil—sillimanite; And—andalusite. (C) Graph of pressure versus south-to-north distance, illustrating decompression paths of the samples shown in A, as constrained by the geochronology of Hallett and Spear (2015) (see the Data Repository for supporting data and a more detailed version of this graph). 'Peak' indicates the maximum pressure that each sample attained. This graph illustrates condensing of structural levels from ~8–11.5 kbar range to ~5–6.5 kbar range between ca. 83–89 Ma and ca. 59–61 Ma.

vertical thinning implied by attenuation of the REH rocks at ~30–43 km depths (Henry et al., 2011) combined with the ~30%–50% vertical thinning at ~15–25 km depths (Camilleri, 1998) defines an upward-decreasing strain gradient (Fig. 3B). Erosion may also have contributed to decompression; however, syn-Cordilleran erosion magnitudes in northeastern Nevada were minimal (~2–3 km; Long, 2012).

ANALOGOUS EXAMPLES

The Himalaya

In the Himalayan orogen, DDT is locally recorded within the Greater Himalayan section, a thick package of amphibolite-facies rocks that were translated southward above the Main Central thrust during the Miocene (e.g., Godin et al., 2006). In several places across the orogen, peak pressures collected through thick sections of Greater Himalayan rocks define upright, super-lithostatic field gradients that have been interpreted as the result of distributed, post–peak metamorphic thinning (Fig. 4B). In central Bhutan, pressures collected from a 10-km-thick section of migmatitic Greater Himalayan rocks and overlying Tethyan Himalayan rocks systematically decrease upward from 10–11.5 kbar to 4.5–6.5 kbar, defining a field gradient of 0.57 ± 0.08 kbar/km, which is ~2× greater than a typical lithostatic gradient of 0.27 kbar/km (Corrie et al., 2012). This was corroborated by finite strain measurements that demonstrate ~40% average, pure shear–dominant, subvertical thinning during ca. 23–15 Ma shearing on the Main Central thrust (Long et al., 2011; 2017). In central Nepal, Larson et al. (2010) documented ~55% post-peak metamorphic vertical thinning (field gradient of 0.62 kbar/km) distributed through a 12 km-thick section of migmatitic Greater Himalayan rocks during early Miocene translation above the Main Central thrust (Fig. 4B). These examples define up to 10–15 km of exhumation (~3–4 kbar of decompression) of the rocks near the base of the thinned interval, entirely as a result of DDT. Overall, DDT accounts for up to 33%–50% of the total exhumation path of these rocks.

Other Orogens

Regions of several other orogenic belts also exhibit evidence for DDT during contractional deformation (see summaries in Ring et al. [1999] and Yonkee [2005]). Examples of high-magnitude DDT at temperatures ≥ 500 °C include 50% thinning in the Sanbagawa belt in Japan, which may have accounted for 15 km of total exhumation (Wallis, 1995), as much as 75% thinning that was likely responsible for 15 km of exhumation in the Betic Cordillera (Spain) (Azañón et al., 1997; Platt et al., 1998), subhorizontal fabric development in Norway's western gneiss region indicating as much as 80% vertical thinning (Dewey et al., 1993), and 66% thinning during nappe emplacement in the Italian Alps that can account for 12 km of exhumation (Ring and Kassem, 2007). Shearing with a large component of subvertical thinning has also been documented in the Caledonian orogen (Europe) (Northrup, 1996; Law, 2010; Thigpen et al., 2010), the Calabrian arc and eastern Alps (Europe) (Wallis et al., 1993), and the Aegean region (Ring and Kumerics, 2008).

DISCUSSION

High-magnitude DDT of thrust sheets during shortening is evident within the ductile portions of many mountain belts and can account for a significant portion of the high-temperature decompression paths of deeply exhumed rocks. Numerous studies attribute such high-temperature decompression to a combination of rapid erosion and/or exhumation by normal faults (e.g., Royden, 1993; Yin, 2006). However, accommodation of DDT implies that neither erosion nor normal faulting is required *a priori*, and plausibly explains *P-T-t* paths from orogens like

[1]GSA Data Repository item 2020105, Figure DR1 (detailed cross-section of the northern East Humboldt Range), Figure DR2 (detailed graph of pressure versus south-to-north distance for samples from the East Humboldt Range), and Table DR1 (published pressure determinations and timing constraints for compiled samples from the northern East Humboldt Range), is available online at http://www.geosociety.org/datarepository/2020/, or on request from editing@geosociety.org.

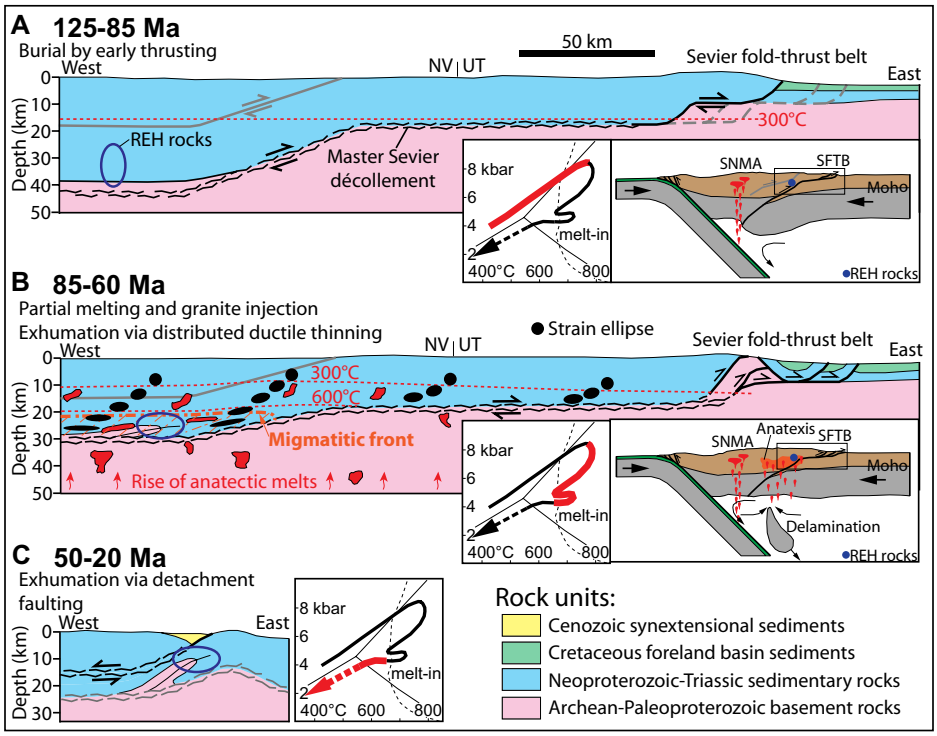

Figure 3. Schematic cross sections of the Cordilleran orogen in Nevada (NV) and Utah (UT), western United States, illustrating the proposed sequence of events in the burial and exhumation history of Ruby–East Humboldt core complex (REH) rocks (pressure-temperature diagrams modified from Hallett and Spear [2015]; inset cross sections modified from Wells et al. [2012]; SNMA—Sierra Nevada magmatic arc; SFTB—Sevier fold-thrust belt). (A) 125–85 Ma: REH rocks were buried to peak temperatures and pressures during early hinterland thrusting (e.g., Camilleri and Chamberlain, 1997). (B) 85–60 Ma: Upward migration of granitic melts following lithospheric delamination elevated isotherms (e.g., Miller and Gans, 1989; Wells and Hoisch, 2008), resulting in partial melting of pelitic rocks at mid-crustal levels. Thermally weakened rocks above basal Sevier décollement underwent distributed ductile thinning during eastward translation, which resulted in decompression. Penetrative strain initiated at temperatures of ~300 °C (e.g., Yonkee, 2005), and increased in magnitude downward with increasing deformation temperature (e.g., Camilleri, 1998), with maximum stretching and thinning within migmatitic rocks (temperatures ≥ 650 °C). Transport-parallel stretching within and above the basal Sevier décollement was fed eastward, likely contributing several tens of kilometers of displacement into the Sevier fold-thrust belt. (C) 50–20 Ma: REH rocks were exhumed via core complex–type extension along a top-down-to-west detachment fault system (e.g., McGrew et al., 2000; Henry et al., 2011). Final exhumation of REH rocks to the surface was accomplished by normal faulting from the middle Miocene to present (e.g., Colgan et al., 2010).

the Cordillera and Himalaya where the hinterland is characterized by broad plateaus that were not significantly eroded or extended.

DDT also explains the development of ubiquitous thrust-subparallel foliations and transport-parallel stretching lineations within exhumed metamorphic terranes (e.g., Ring et al., 1999). Hotter, weaker rocks lose their ability to transmit significant shear traction, which results in increasing components of pure shear–dominant, thrust-normal thinning and transport-parallel stretching (e.g., Means, 1989; Camilleri, 1998; Yonkee, 2005; Law et al., 2013). In quartz-rich rocks, DDT initiates at deformation temperatures of ~300 °C (e.g., Stipp et al., 2002; Yonkee, 2005; Long et al., 2011), with strain magnitude expected to increase with increasing deformation temperature (e.g., Ring and Kassem, 2007). This implies that the basal décollements of brittle thrust systems likely become stretching faults (Means, 1989) as they cut deeply beneath the hinterland, which has far-reaching implications for mass transfer in orogenic systems and for the kinematic relationships between hinterland and foreland deformation.

As a condition of strain compatibility, in the absence of major upper-crustal normal faulting, transport-parallel stretching at deep levels must be balanced by horizontal shortening and vertical thickening in the frontal fold-thrust belt (e.g., Williams et al., 2006; Larson et al., 2010). The overall upward decrease in transport-parallel stretching of the thinned interval could be accommodated either by a discrete normal-sense shear zone, such as the Himalayan South Tibetan detachment system (e.g., Northrup, 1996), or alternatively by a distributed vertical gradient in transport-parallel stretching (Figs. 1A and 3B), such as documented in the Wood Hills and Pequop Mountains in Nevada by Camilleri (1998). For the case of the U.S. Cordillera, where synorogenic upper-crustal normal faulting was minimal (e.g., Henry et al., 2011), we propose that transport-parallel stretching under the hinterland was kinematically linked to shortening in the Sevier thrust belt (Fig. 3B). Consequently, a portion (perhaps several tens of kilometers) of the 150–220 km of shortening in the Sevier thrust belt can likely be attributed to enhanced eastward displacement generated by stretching above the master décollement. Therefore, transport-parallel stretching accompanying DDT is an important component of the deformation field that must be considered for accurate orogenic mass-balance assessment.

ACKNOWLEDGMENTS

This work was funded by U.S. National Science Foundation grants EAR-1450507 and OIA-1545903 awarded to Kohn, and EAR-1220300 awarded to Long. This study has benefitted from discussions with many outstanding western United States geologists, including Chris Henry, Joe Colgan, Jeffrey Lee, and Elizabeth Miller. Additionally, many ideas in this paper were inspired by the work of several excellent Himalayan structural geologists, including Richard Law, Laurent Godin, Kyle Larson, Micah Jessup, and Djordje Grujic. We thank Uwe Ring, Richard Law, and an anonymous reviewer for constructive reviews of this paper.

REFERENCES CITED

Azañón, J.M., Crespo-Blanc, A., and García-Dueñas, V., 1997, Continental collision, crustal thinning and nappe forming during the pre-Miocene evolution of the Alpujarride Complex (Alboran Domain, Betics): Journal of Structural Geology, v. 19, p. 1055–1071, https://doi.org/10.1016/S0191-8141(97)00031-X.

Camilleri, P.A., 1998, Prograde metamorphism, strain evolution, and collapse of footwalls of thick thrust sheets: A case study from the Mesozoic Sevier hinterland U.S.A.: Journal of Structural Geology, v. 20, p. 1023–1042, https://doi.org/10.1016/S0191-8141(98)00032-7.

Camilleri, P.A., and Chamberlain, K.R., 1997, Mesozoic tectonics and metamorphism in the Pequop Mountains and Wood Hills region, northeast Nevada: Implications for the architecture and evolution of the Sevier orogen: Geological Society of America Bulletin, v. 109, p. 74–94, https://doi.org/10.1130/0016-7606(1997)109<0074:MTAMIT>2.3.CO;2.

Colgan, J.P., Howard, K.A., Fleck, R.J., and Wooden, J.L., 2010, Rapid middle Miocene extension and unroofing of the southern Ruby Mountains, Nevada: Tectonics, v. 29, TC6022, https://doi.org/10.1029/2009TC002655.

Coney, P.J., and Harms, T.J., 1984, Cordilleran metamorphic core complexes: Cenozoic extensional relics of Mesozoic compression: Geology, v. 12, p. 550–554, https://doi.org/10.1130/0091-7613(1984)12<550:CMCCCE>2.0.CO;2.

Corrie, S.L., Kohn, M.J., McQuarrie, N., and Long, S.P., 2012, Flattening the Bhutan Himalaya: Earth and Planetary Science Letters, v. 349–350, p. 67–74, https://doi.org/10.1016/j.epsl.2012.07.001.

DeCelles, P.G., 2004, Late Jurassic to Eocene evolution of the Cordilleran thrust belt and foreland basin system, western U.S.A.: American Journal of Science, v. 304, p. 105–168, https://doi.org/10.2475/ajs.304.2.105.

Dewey, J.F., Ryan, P.D., and Andersen, T.B., 1993, Orogenic uplift and collapse, crustal thickness,

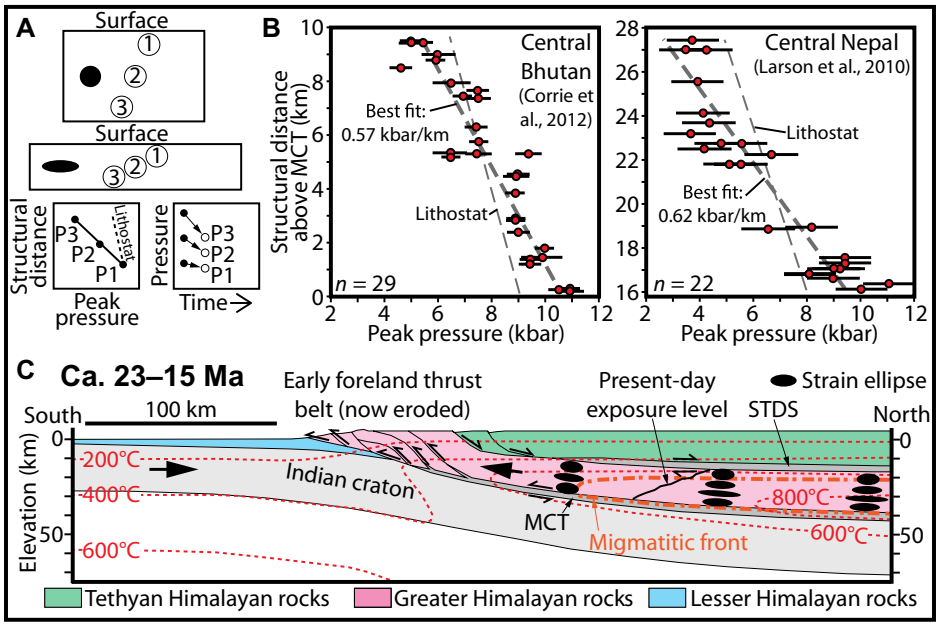

Figure 4. (A) Diagrams illustrating the consequences of post–peak metamorphic, pure shear–dominated distributed ductile thinning (DDT) of a subhorizontal thrust sheet, which is expected to yield a super-lithostatic peak pressure gradient (modified from Corrie et al., 2012). Decompression is predicted to be greatest toward the bottom of the thrust sheet. 1, 2, and 3 represent high, middle, and low structural positions within the thrust sheet, respectively, and P1, P2, and P3 represent corresponding peak pressures of these three positions. The line labeled 'Lithostat' represents a lithostatic pressure gradient. (B) Examples of peak pressure distributions from samples collected from the Main Central thrust (MCT) sheet in central Bhutan (Corrie et al., 2012) and central Nepal (Larson et al., 2010). These data define super-lithostatic baric field gradients, which were interpreted to have been produced by distributed post–peak metamorphic thinning of the MCT sheet during southward translation. (C) Schematic cross section of the Himalayan orogen, illustrating the evolution of deformation during the southward translation of the MCT sheet between ca. 23 and 15 Ma (isotherms after Henry et al., 1997). DDT within mid-crustal Greater Himalayan rocks between the MCT and South Tibetan detachment system (STDS) locally resulted in decompression. Transport-parallel stretching along and above the MCT (e.g., Long et al., 2016, 2017) likely contributed displacement southward into an early, brittle foreland fold-thrust belt, which has now been removed by erosion.

fabrics and metamorphic phase changes: The role of eclogites, *in* Prichard, H.M., et al., eds., Magmatic Processes and Plate Tectonics: Geological Society of London Special Publication 76, p. 325–343, https://doi.org/10.1144/GSL.SP.1993.076.01.16.

England, P., and Molnar, P., 1990, Surface uplift, uplift of rocks, and exhumation of rocks: Geology, v. 18, p. 1173–1177, https://doi.org/10.1130/0091-7613(1990)018<1173:SUURA>2.3.CO;2.

Feehan, J.G., and Brandon, M.T., 1999, Contribution of ductile flow to exhumation of low-temperature, high-pressure metamorphic rocks: San Juan–Cascade nappes, NW Washington State: Journal of Geophysical Research, v. 104, p. 10,883–10,902, https://doi.org/10.1029/1998JB900054.

Godin, L., Grujic, D., Law, R.D., and Searle, M.P., 2006, Channel flow, ductile extrusion and exhumation in continental collision zones: An introduction, *in* Law, R.D., et al., eds., Channel Flow, Ductile Extrusion and Exhumation in Continental Collision Zones: Geological Society of London Special Publication 268, p. 1–23, https://doi.org/10.1144/GSL.SP.2006.268.01.01.

Hallett, B.W., and Spear, F.S., 2014, The *P-T* history of anatectic pelites of the northern East Humboldt Range, Nevada: Evidence for tectonic loading, decompression, and anatexis: Journal of Petrology, v. 55, p. 3–36, https://doi.org/10.1093/petrology/egt057.

Hallett, B.W., and Spear, F.S., 2015, Monazite, zircon, and garnet growth in migmatitic pelites as a record of metamorphism and partial melting in the East Humboldt Range, Nevada: American Mineralogist, v. 100, p. 951–972, https://doi.org/10.2138/am-2015-4839.

Henry, C.D., McGrew, A.J., Colgan, J.P., Snoke, A.W., and Brueseke, M.E., 2011, Timing, distribution, amount, and style of Cenozoic extension in the northern Great Basin, *in* Lee, J., and Evans, J.P., eds., Geologic Field Trips to the Basin and Range, Rocky Mountains, Snake River Plain, and Terranes of the U.S. Cordillera: Geological Society of America Field Guide 21, p. 27–66, https://doi.org/10.1130/2011.0021(02).

Henry, P., LePichon, X., and Goffé, B., 1997, Kinematic, thermal and petrological model of the Himalayas: Constraints related to metamorphism within the underthrust Indian crust and topographic elevation: Tectonophysics, v. 273, p. 31–56, https://doi.org/10.1016/S0040-1951(96)00287-9.

Hodges, K.V., Snoke, A.W., and Hurlow, H.A., 1992, Thermal evolution of a portion of the Sevier hinterland: The northern Ruby Mountains–East Humboldt Range and Wood Hills, northeastern Nevada: Tectonics, v. 11, p. 154–164, https://doi.org/10.1029/91TC01879.

Larson, K.P., Godin, L., and Price, R.A., 2010, Relationships between displacement and distortion in orogens: Linking the Himalayan foreland and hinterland in central Nepal: Geological Society of America Bulletin, v. 122, p. 1116–1134, https://doi.org/10.1130/B30073.1.

Law, R.D., 2010, Moine Thrust zone mylonites at the Stack of Glencoul: II—Results of vorticity analyses and their tectonic significance, *in* Law, R.D., et al., eds., Continental Tectonics and Mountain Building—The Legacy of Peach and Horne: Geological Society of London Special Publication 335, p. 579–602, https://doi.org/10.1144/SP335.24.

Law, R.D., Stahr, D.W., III, Francsis, M.K., Ashley, K.T., Grasemann, B., and Ahmad, T., 2013, Deformation temperatures and flow vorticities near the base of the Greater Himalayan Series, Sutlej Valley and Shimla Klippe, NW India: Journal of Structural Geology, v. 54, p. 21–53, https://doi.org/10.1016/j.jsg.2013.05.009.

Long, S.P., 2012, Magnitudes and spatial patterns of erosional exhumation in the Sevier hinterland, eastern Nevada and western Utah, USA: Insights from a Paleogene paleogeologic map: Geosphere, v. 8, p. 881–901, https://doi.org/10.1130/GES00783.1.

Long, S.P., and Soignard, E., 2016, Shallow-crustal metamorphism during Late Cretaceous anatexis in the Sevier hinterland plateau: Peak temperature conditions from the Grant Range, eastern Nevada, U.S.A.: Lithosphere, v. 8, p. 150–164, https://doi.org/10.1130/L501.1.

Long, S., McQuarrie, N., Tobgay, T., and Hawthorne, J., 2011, Quantifying internal strain and deformation temperature in the eastern Himalaya, Bhutan: Implications for the evolution of strain in thrust sheets: Journal of Structural Geology, v. 33, p. 579–608, https://doi.org/10.1016/j.jsg.2010.12.011.

Long, S.P., Gordon, S.M., Young, J.P., and Soignard, E., 2016, Temperature and strain gradients through Lesser Himalayan rocks and across the Main Central thrust, south-central Bhutan: Implications for transport-parallel stretching and inverted metamorphism: Tectonics, v. 35, p. 1863–1891, https://doi.org/10.1002/2016TC004242.

Long, S.P., Gordon, S.M., and Soignard, E., 2017, Distributed north-vergent shear and flattening through Greater and Tethyan Himalayan rocks: Insights from metamorphic and strain data from the Dang Chu region, central Bhutan: Lithosphere, v. 9, p. 774–795, https://doi.org/10.1130/L655.1.

McGrew, A.J., Peters, M.T., and Wright, J.E., 2000, Thermobarometric constraints on the tectonothermal evolution of the East Humboldt Range metamorphic core complex, Nevada: Geological Society of America Bulletin, v. 112, p. 45–60, https://doi.org/10.1130/0016-7606(2000)112<45:TCOTTE>2.0.CO;2.

McQuarrie, N., and Wernicke, B.P., 2005, An animated tectonic reconstruction of southwestern North America since 36 Ma: Geosphere, v. 1, p. 147–172, https://doi.org/10.1130/GES00016.1.

Means, W.D., 1989, Stretching faults: Geology, v. 17, p. 893–896, https://doi.org/10.1130/0091-7613(1989)017<0893:SF>2.3.CO;2.

Miller, E.L., and Gans, P.B., 1989, Cretaceous crustal structure and metamorphism in the hinterland of the Sevier thrust belt, western U.S. Cordillera: Geology, v. 17, p. 59–62, https://doi.org/10.1130/0091-7613(1989)017<0059:CCSAMI>2.3.CO;2.

Northrup, C.J., 1996, Structural expressions and tectonic implications of general noncoaxial flow in the midcrust of a collisional orogen: The northern Scandinavian Caledonides: Tectonics, v. 15, p. 490–505, https://doi.org/10.1029/95TC02951.

Peters, M.T., and Wickham, S.M., 1994, Petrology of upper amphibolite facies marbles from the East

Humboldt Range, Nevada, USA: Evidence for high-temperature, retrograde, hydrous volatile fluxes at mid-crustal levels: Journal of Petrology, v. 35, p. 205–238, https://doi.org/10.1093/petrology/35.1.205.

Platt, J.P., 1993, Exhumation of high-pressure rocks: A review of concepts and processes: Terra Nova, v. 5, p. 119–133, https://doi.org/10.1111/j.1365-3121.1993.tb00237.x.

Platt, J.P., Soto, J.I., Whitehouse, M.J., Hurford, A.J., and Kelley, S.P., 1998, Thermal evolution, rate of exhumation, and tectonic significance of metamorphic rocks from the floor of the Alboran extensional basin, western Mediterranean: Tectonics, v. 17, p. 671–689, https://doi.org/10.1029/98TC02204.

Ring, U., and Kassem, O.M.K., 2007, The nappe rule: Why does it work?: Journal of the Geological Society, v. 164, p. 1109–1112, https://doi.org/10.1144/0016-76492007-020.

Ring, U., and Kumerics, C., 2008, Vertical ductile thinning and its contribution to the exhumation of high-pressure rocks: The Cycladic blueschist unit in the Aegean: Journal of the Geological Society, v. 165, p. 1019–1030, https://doi.org/10.1144/0016-76492008-010.

Ring, U., Brandon, M.T., Willett, S.D., and Lister, G.S., 1999, Exhumation processes, *in* Ring, U., et al., eds., Exhumation Processes: Normal Faulting, Ductile Flow and Erosion: Geological Society of London Special Publication 154, p. 1–27, https://doi.org/10.1144/GSL.SP.1999.154.01.01.

Rosenberg, C.L., and Handy, M.R., 2005, Experimental deformation of partially melted granite revisited: Implications for the continental crust: Journal of Metamorphic Geology, v. 23, p. 19–28, https://doi.org/10.1111/j.1525-1314.2005.00555.x.

Royden, L.H., 1993, The steady state thermal structure of eroding orogenic belts and accretionary prisms: Journal of Geophysical Research, v. 98, p. 4487–4507, https://doi.org/10.1029/92JB01954.

Stipp, M., Stünitz, H., Heilbronner, R., and Schmid, S.M., 2002, The eastern Tonale fault zone: A 'natural laboratory' for crystal plastic deformation over a temperature range from 250 to 700 °C: Journal of Structural Geology, v. 24, p. 1861–1884, https://doi.org/10.1016/S0191-8141(02)00035-4.

Thigpen, J.R., Law, R.D., Lloyd, G.E., Brown, S.J., and Cook, B., 2010, Deformation temperatures, vorticity of flow and strain symmetry in the Loch Eriboll mylonites, NW Scotland: Implications for the kinematic and structural evolution of the northernmost Moine Thrust zone, *in* Law, R.D., et al., eds., Continental Tectonics and Mountain Building—The Legacy of Peach and Horne: Geological Society of London Special Publication 335, p. 623–662, https://doi.org/10.1144/SP335.26.

Wallis, S.R., 1995, Vorticity analysis and recognition of ductile extension in the Sanbagawa belt, SW Japan: Journal of Structural Geology, v. 17, p. 1077–1093, https://doi.org/10.1016/0191-8141(95)00005-X.

Wallis, S.R., Platt, J.P., and Knott, S.D., 1993, Recognition of synconvergence extension in accretionary wedges with examples from the Calabrian Arc and the Eastern Alps: American Journal of Science, v. 293, p. 463–494, https://doi.org/10.2475/ajs.293.5.463.

Wells, M.L., and Hoisch, T.D., 2008, The role of mantle delamination in widespread Late Cretaceous extension and magmatism in the Cordilleran orogen, western United States: Geological Society of America Bulletin, v. 120, p. 515–530, https://doi.org/10.1130/B26006.1.

Wells, M.L., Hoisch, T.D., Cruz-Aribe, A.M., and Vervoort, J.D., 2012, Geodynamics of synconvergent extension and tectonic mode switching: Constraints from the Sevier-Laramide orogeny: Tectonics, v. 31, TC1002, https://doi.org/10.1029/2011TC002913.

Wernicke, B., and Burchfiel, B.C., 1982, Modes of extensional tectonics: Journal of Structural Geology, v. 4, p. 105–115, https://doi.org/10.1016/0191-8141(82)90021-9.

Willett, S.D., and Brandon, M.T., 2002, On steady states in mountain belts: Geology, v. 30, p. 175–178, https://doi.org/10.1130/0091-7613(2002)030<0175:OSSIMB>2.0.CO;2.

Williams, P.F., Jiang, D., and Lin, S., 2006, Interpretation of deformation fabrics of infrastructure zone rocks in the context of channel flow and other tectonic models, *in* Law, R.D., et al., eds., Channel Flow, Ductile Extrusion and Exhumation in Continental Collision Zones: Geological Society of London Special Publication 268, p. 221–235, https://doi.org/10.1144/GSL.SP.2006.268.01.10.

Yin, A., 2006, Cenozoic tectonic evolution of the Himalayan orogen as constrained by along-strike variation of structural geometry, exhumation history, and foreland sedimentation: Earth-Science Reviews, v. 76, p. 1–131, https://doi.org/10.1016/j.earscirev.2005.05.004.

Yonkee, A., 2005, Strain patterns within part of the Willard thrust sheet, Idaho-Wyoming-Utah thrust belt: Journal of Structural Geology, v. 27, p. 1315–1343, https://doi.org/10.1016/j.jsg.2004.06.014.

Yonkee, W.A., and Weil, A.B., 2015, Tectonic evolution of the Sevier and Laramide belts within the North American Cordillera orogenic system: Earth-Science Reviews, v. 150, p. 531–593, https://doi.org/10.1016/j.earscirev.2015.08.001.

Printed in USA